

## Anisotropic electrical resistivity of ferromagnetic Co-Pd and Co-Pt alloys

H. Ebert and A. Vernes

*Institut für Physikalische Chemie, Universität München, Theresienstraße 37, D-80333 München, Germany*

John Banhart

*Fraunhofer-Institut für Angewandte Materialforschung, Lesumer Heerstraße 36, D-28717 Bremen, Germany*

(Received 13 March 1996)

First-principles calculations of the electrical conductivity of disordered ferromagnetic alloys based on the Kubo-Greenwood formalism and the spin-polarized relativistic Korringa-Kohn-Rostoker coherent-potential-approximations method are presented. Application to the alloy systems Co-Pd and Co-Pt yields results for the isotropic and anisotropic residual resistivity which are in very satisfying agreement with experiment. In addition, scalar-relativistic calculations of the isotropic residual resistivity were performed on the basis of the two-current model for these alloy systems, and were found to agree with the relativistic results fairly well. [S0163-1829(96)01336-7]

### I. INTRODUCTION

The transport properties of ferromagnetic alloys show a remarkable feature: their resistivity depends on the direction of the electrical current with respect to the direction of spontaneous magnetization even for a vanishing external magnetic field. This behavior is reflected by the shape of the resistivity tensor, which for cubic systems with a magnetization vector in the  $z$  direction takes the form<sup>1</sup>

$$\rho = \sigma^{-1} = \begin{pmatrix} \rho_{\perp} & -\rho_H & 0 \\ \rho_H & \rho_{\perp} & 0 \\ 0 & 0 & \rho_{\parallel} \end{pmatrix}, \quad (1)$$

with  $\rho_{\perp}$  and  $\rho_{\parallel}$  being the transverse and longitudinal resistivities, respectively. The off-diagonal element  $\rho_H$  represents the spontaneous or anomalous Hall resistivity,<sup>2</sup> which shall not be considered in the present paper. The spontaneous magnetoresistance anisotropy (SMA) is defined by<sup>1</sup>

$$\frac{\Delta\rho}{\bar{\rho}} = \frac{\rho_{\parallel}(B) - \rho_{\perp}(B)}{\bar{\rho}(B)} \Big|_{B \rightarrow 0}, \quad (2)$$

where  $\bar{\rho} = \frac{1}{3}(2\rho_{\perp} + \rho_{\parallel})$  is the isotropic resistivity. Experimentally the SMA is found by measuring  $\rho_{\parallel}(B)$  and  $\rho_{\perp}(B)$  as functions of the applied magnetic field  $B$ , and by subsequent extrapolation to  $B=0$ . In general, the electrical resistivity is found to be higher for the current aligned parallel to the magnetization than for the current perpendicular to the magnetization (i.e.,  $\rho_{\parallel} > \rho_{\perp}$ ), but the opposite situation is also encountered in a few cases.<sup>3</sup>

It is important to note that the SMA as defined in Eq. (2) must not be confused with the conventional magnetoresistance which is defined as a  $B$ -dependent function  $\Delta\rho/\rho = [\rho(B) - \rho(0)]/\rho(0)$ . In contrast to this situation, the external magnetic field here is applied just to align the spontaneous magnetization.

The interest in the anisotropic resistivity is of twofold origin: first there are important technological applications for

the effect such as, for example, for magnetic recording devices.<sup>4,5</sup> Here the goal is to find alloys which exhibit large SMA ratios at room temperature, and which can be prepared as thin films. On the other hand, the effect is interesting from a theoretical viewpoint: unlike the conventional magnetoresistance which is due to the Lorentz forces acting directly on the conduction electrons, the SMA cannot be explained this way. The reason for the occurrence of a resistance anisotropy even for vanishing magnetic fields must be seen in the reduced symmetry of the crystal lattice due to the alignment of the magnetic moments. The scattering of the electrons then depends on the angle between the current and the magnetization vector because of the spin-orbit interaction.<sup>6</sup>

Smit<sup>6</sup> and later Campbell and co-workers<sup>7,8</sup> carried out a series of investigations on nickel-based alloys which exhibit very high anisotropy ratios for low temperatures, and applied the two-current model of electrical conduction in order to explain the SMA. However, more recent theoretical investigations of nickel alloys, and here mainly the system Fe-Ni, seem to indicate that the two current model does not work very well for these alloy systems<sup>2,9,10</sup> because of an unusually low scattering rate in the majority-spin band. In contrast, the alloy Co-Pd, which also has a high SMA and has recently attracted attention of experimentalists,<sup>11-14</sup> is expected to be more suited to be described in terms of the two-current model. We have chosen this alloy system as well as the system Co-Pt in order to test the recently developed method of first-principles calculation of anisotropical transport coefficients, allowing also for an assessment of the two-current model.

### II. THEORETICAL FRAMEWORK

A straightforward and rigorous access to galvanomagnetic effects is supplied by the Kubo-Greenwood equation for the conductivity tensor  $\sigma$ ,<sup>15,16</sup>

$$\sigma_{\mu\nu} = \frac{\hbar}{\pi V_{\text{cryst}}} \text{Tr} \langle j_{\mu} \text{Im} G^{+}(E_F) j_{\nu} \text{Im} G^{+}(E_F) \rangle_{\text{conf.}} \quad (3)$$

Here  $G^+(E_F)$ , representing the electronic structure of the system, is the positive side limit of the single-particle Green function at the Fermi energy  $E_F$ ,  $j_\mu$  is the  $\mu$ th spatial component of the electronic current operator  $j$ , and  $\langle \rangle_{\text{conf.}}$  denotes the atomic configuration average for a disordered alloy. A very accurate determination of the electronic Green function  $G^+(\mathbf{r}, \mathbf{r}', E)$  in real space is achieved by using the Korringa-Kohn-Rostoker (KKR) method of band-structure calculation or, in other words, on the basis of multiple-scattering theory:

$$\text{Im}G(\mathbf{r}, \mathbf{r}', E) = \sum_{L, L'} Z_L(\mathbf{r}, E) \tau_{L, L'}(E) Z_{L'}^\dagger(\mathbf{r}', E). \quad (4)$$

Here  $Z_L(\mathbf{r}, E)$  is the regular solution to the Schrödinger equation (or Dirac equation; see below), and  $\tau_{L, L'}(E)$  is the scattering path operator — the central quantity of multiple-scattering theory. To deal with a randomly disordered alloy the corresponding configurational average of the Green function is obtained in a most reliable way by using the coherent-potential-approximation (CPA) alloy theory. This single-site theory ignores any correlation in the occupation of neighboring atomic sites, i.e., atomic short-range order, and aims to supply a hypothetical ordered CPA medium that represents the configurationally averaged electronic properties of a disordered alloy. Within the multiple scattering formalism, the CPA medium is described by its single-site  $t$  matrix  $t^{\text{CPA}}$  and its scattering path operator  $\tau^{\text{CPA}}$ , and specifying the CPA medium consists in solving the CPA equations

$$\begin{aligned} \tau^{\text{CPA}} &= \frac{1}{\Omega_{\text{BZ}}} \int_{\Omega_{\text{BZ}}} d^3k [(t^{\text{CPA}})^{-1} - G(\mathbf{k}, E)]^{-1}, \\ \tau^{\text{CPA}} &= x \tau^{\text{A}} + (1-x) \tau^{\text{B}}, \\ \tau^{\text{A}} &= [(t^{\text{A}})^{-1} - (t^{\text{CPA}})^{-1} + (\tau^{\text{A}})^{-1}]^{-1}. \end{aligned} \quad (5)$$

Here an alloy  $A_x B_{1-x}$  has been assumed, and use has been made of the fact that the CPA medium is ordered, and  $\tau^{\text{CPA}}$  can be determined by a Brillouin-zone integral with  $G(\mathbf{k}, E)$  the so-called KKR-structure constants.

Having determined the electronic Green function  $G^+(\mathbf{r}, \mathbf{r}', E)$ , Eq. (3) can be evaluated in a rather straightforward way. For paramagnetic systems the corresponding expression for  $\sigma_{\mu\nu}$  has been worked out in great detail by Butler.<sup>16</sup> In particular he has shown how to deal with the configurational average of the product of two Green functions in the framework of the CPA, that primarily deals with the configurational average of one Green function. The expressions derived by Butler have been applied so far with great success in their original nonrelativistic form<sup>17</sup> as well as their corresponding fully relativistic form<sup>18</sup> to calculate the residual resistivity of various alloy systems.

To obtain access to the SMA in the limit  $T=0$  K, Butler's approach was generalized recently<sup>2</sup> by evaluating  $G^+(E_F)$  using the spin-polarized relativistic version of the KKR-CPA (SPR-KKR-CPA).<sup>19</sup> This scheme, based on the Dirac equation for a spin-dependent potential derived from local spin-density-functional theory, accounts on the same level — without using any parameters — for all relativistic effects as well as for the magnetic state. A direct consequence of this is that the symmetry reduction due to the simultaneous presence of spin-orbit interaction and magnetism — giving rise

to the form of  $\rho$  in Eq. (1) — is automatically accounted for. Finally, one has to mention that using the SPR-KKR-CPA there is no need to rely on the two-current model anymore. This is the case because the SPR-KKR formalism accounts in a natural way for the fact that the electronic states have in general no unique spin character. Therefore, no artificial subdivision of the electronic current into spin-up and -down parts has to be assumed. Nevertheless, whenever it is possible and sensible in the following, the residual conductivity of the investigated alloy systems will be discussed on the basis of the spin-projected electronic structure.

### III. RESULTS AND DISCUSSION

#### A. Electronic structure

To provide the basis for the calculation of the conductivity tensor (see above) the electronic structure of a series of Co-Pd and Co-Pt randomly disordered alloys has been calculated using the SPR-KKR-CPA method of band-structure calculation.<sup>19</sup> All these calculations have been performed using potentials that have been created within the framework of local spin-density-functional theory<sup>20</sup> in a scalar-relativistic way, i.e., omitting the spin-orbit coupling. As representative examples for the results of the SPR-KKR-CPA calculations, that account for the spin-orbit coupling, the spin-projected density-of-states (DOS) curves for  $\text{Co}_{40}\text{Pd}_{60}$  and  $\text{Co}_{40}\text{Pt}_{60}$  are given in Fig. 1. For both systems the partial DOS of Co is strongly exchange split, with a corresponding magnetic moment that increases monotonously with decreasing Co concentration.<sup>19</sup> For Pd and Pt, the hybridization with Co states also gives rise to a small exchange splitting for these components, resulting in an induced spin magnetic moment of some tenth of a Bohr magneton.<sup>19</sup> The main difference between the systems Co-Pd and Co-Pt is obviously the widths of the Pd and Pt  $d$  bands. The higher  $d$ -band width in the case of Co-Pt is due to the fact that the  $d$ -wave functions of Pt are less localized than those of Pd and, to a lesser extent, due to the higher spin-orbit coupling strength of Pt. A consequence of the higher  $d$ -band-width of Pt, compared to Pd, is the weaker hybridization with Co states and a smaller resulting spin magnetic moment. However, more important for the conductivity is the influence on the DOS at the Fermi energy. As can be seen in Fig. 2, the difference for the spin-resolved DOS at the Fermi energy,  $n^\downarrow(E_F)$  and  $n^\uparrow(E_F)$ , respectively, decreases much faster for Co-Pt than for Co-Pd as function of concentration. As will be discussed below, this will have important consequences for the isotropic resistivity  $\bar{\rho}$  as well as the SMA ratio  $\Delta\rho/\bar{\rho}$  for these alloy systems.

#### B. Relativistic calculation of transport properties

The fully relativistic treatment of the electrical conductivity or resistivity, respectively, yields a tensor which is reduced in symmetry, thus reflecting the presence of magnetic ordering [see Eq. (1)]. Averaging the diagonal components of this tensor gives the isotropic resistivity  $\bar{\rho}$  which can be compared to the experimental resistivity measured on magnetically saturated polycrystalline samples, whereas the difference between the diagonal components is a measure of the SMA according to the definition in Eq. (2). All calculations

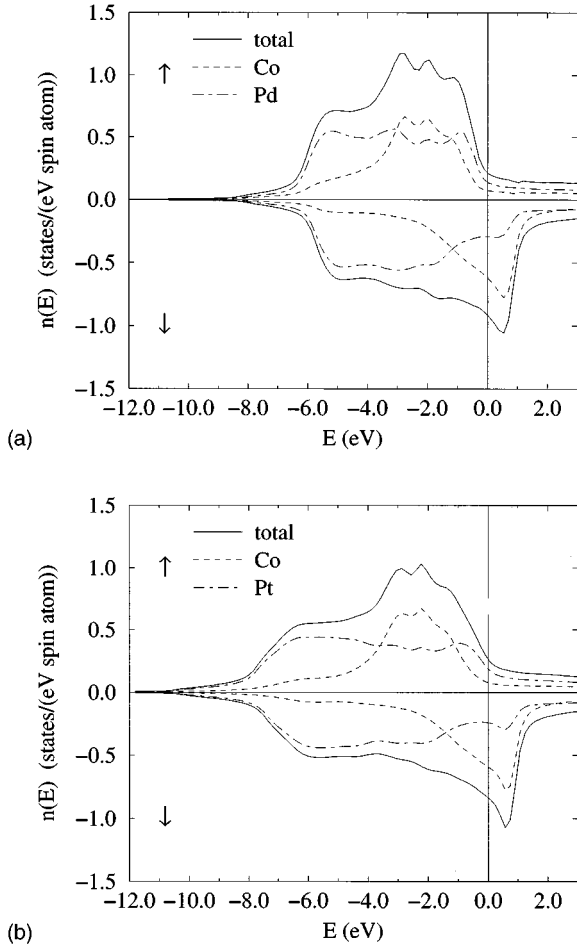


FIG. 1. Spin-projected density of states for  $\text{Co}_{40}\text{Pd}_{60}$  (top) and  $\text{Co}_{40}\text{Pt}_{60}$  (bottom) calculated using the SPR-KKR-CPA method.

presented in the following were carried out including angular momenta up to  $\ell_{\text{max}}=3$  in the angular momentum expansion in Eq. (4). The Brillouin-zone integration in Eq. (5) as well as in that connected with Eq. (3) has been evaluated using a special direction method in  $\mathbf{k}$  space<sup>21</sup> with a very fine grid to ensure the convergency. In all calculations the vertex corrections,<sup>16</sup> that account for the difference of Eq. (3) and

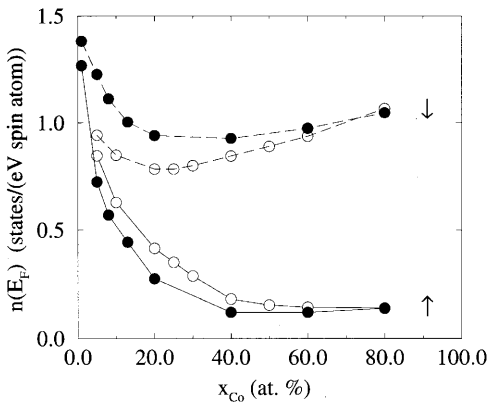


FIG. 2. Spin-projected density of states  $n(E_F)$  at the Fermi energy level for Co-Pd (●) and Co-Pt (○) calculated for the two-spin bands in the scalar relativistic way. Full line: majority spin; dashed line: minority spin.

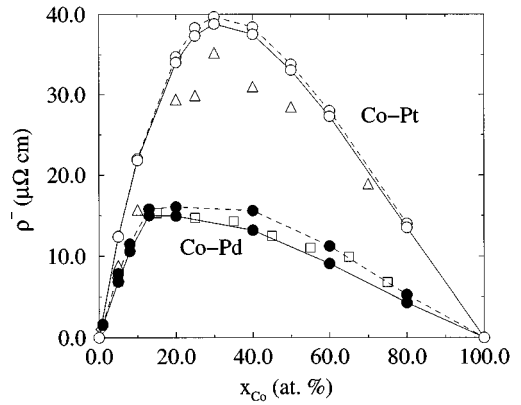


FIG. 3. Residual isotropic resistivity  $\bar{\rho}$  of disordered Co-Pd (●) and Co-Pt (○) alloys. Full lines: calculated including vertex corrections; broken lines: calculated omitting vertex corrections. Experimental values for Co-Pd were taken from Refs. 11 and 12 (□) and Ref. 22 (◇), and for Co-Pt from Ref. 14 (△).

its simplified version with the average of the product of two Green functions replaced by the product of two averaged Green functions, were included. This description of the calculations also apply to those performed in a scalar-relativistic way without spin-orbit coupling (see below). Further technical details can be found in Ref. 18.

### 1. Isotropic resistivity

The calculated isotropic resistivities for the alloy systems Co-Pd and Co-Pt are shown in Fig. 3. Also included are from various sources, the corresponding experimental data measured at low temperature.

Obviously, the agreement between calculated and measured resistivities is very good for Co-Pd. The maximum value of the resistivity in this system (16  $\mu\Omega \text{ cm}$ ) as well as the composition for which the maximum occurs (about 20% Co) are well reproduced by the calculations. The proper treatment of angular momenta up to  $\ell_{\text{max}}=3$  is essential for this result, because an angular momentum expansion with  $\ell_{\text{max}}=2$  leads to much higher resistivities. As mentioned, the calculations include the vertex corrections. It was found that their contribution increases from about 2% for 5 at. % Co to about 25% for 80 at. % Co.

For the system Co-Pt the calculated resistivities are much higher than for Co-Pd, reaching almost 40  $\mu\Omega \text{ cm}$  for 30 at. % Co. This agrees in a satisfactory way with the experimental maximum of about 35  $\mu\Omega \text{ cm}$  at that composition. As for Co-Pd inclusion of  $f$  states is important. The relative difference  $1 - \bar{\rho}_2/\bar{\rho}_3$ , where  $\bar{\rho}_\ell$  is the calculated residual resistivity with angular momenta up to  $\ell$  included, drops from 0.59 to 0.31 as one goes from 5 to 80 at. % Co.

For Co-Pt the vertex corrections are quite small, contributing less than 3% to the total conductivity over the entire composition range. From the experience with paramagnetic alloy systems,<sup>18</sup> one can conclude that for this case the vertex corrections are the more important the lower the  $d$  DOS at the Fermi level is. For Cu-Pt,<sup>18</sup> for example, this applies to the noble-metal-rich side of this system. For ferromagnetic systems, on the other hand, the vertex corrections seem to be more important, if the  $d$  DOS at the Fermi level is low at

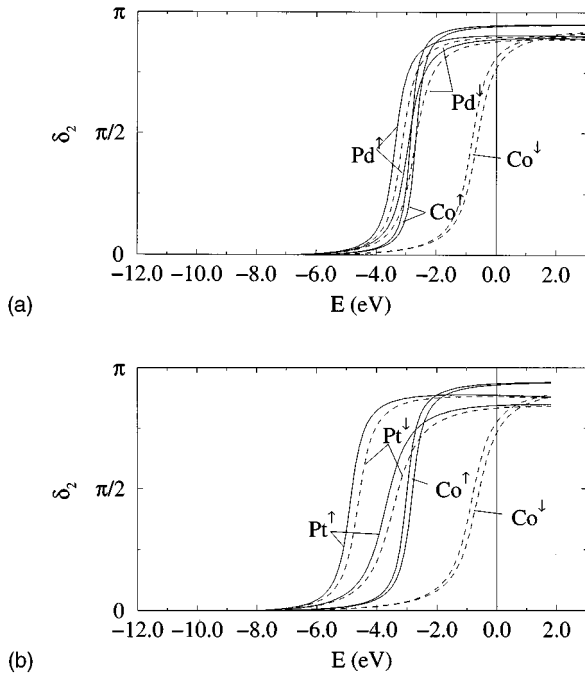


FIG. 4. Phase shifts  $\delta_2$  for  $d_{3/2}$  and  $d_{5/2}$  states of Co, Pd, and Pt in  $\text{Co}_{20}\text{Pd}_{80}$  (top) and  $\text{Co}_{30}\text{Pt}_{70}$  (bottom), respectively, calculated using the potentials for spin-up (full curves) and -down (dashed curves). The difference of the resonance position for the  $d_{3/2}$  (lower energy) and  $d_{5/2}$  states (higher energy) can be taken as a measure for the corresponding spin-orbit coupling strength.

least for one spin subsystem (see also the discussion below of the two-current model). For this reason, they are more pronounced for Co-Pd compared to Co-Pt, and more important on the Co-rich side of both systems (compare Fig. 2).

The reason for the higher residual resistivity of Co-Pt as compared to Co-Pd can be made clear with the help of the scattering phase shifts  $\delta_2$  for the  $d$  electrons. These quantities determine the position and width of the  $d$  bands (see Fig. 1) and have a resonancelike shape for transition metals. For the spin-polarized relativistic situation, this quantity should, in principle, be represented by a matrix. However, to obtain an impression of the relative importance of the exchange and spin-orbit splitting, the phase shifts for  $d_{3/2}$  and  $d_{5/2}$  states have been calculated by solving the radial Dirac equations using the potentials for spin-up and -down, separately. For the majority-spin system the phase shifts of Co and Pd in Co-Pd are very similar in position and width (see Fig. 4). For that reason, there is not much scatter due to chemical disorder. As a consequence a rather small resistivity can be expected. For the minority-spin system, on the other hand, the phase shifts for Co and Pd are quite different because of the different exchange splitting. For that reason a stronger scattering due to chemical disorder and in turn an enhancement of the total resistivity can be expected. For Co-Pt the situation is quite different from that for Co-Pd. Here the position of the phase-shift resonance differs in position because of the strong exchange splitting for Co and the strong spin-orbit splitting for Pt. Thus stronger scattering due to chemical disorder and therefore a higher isotropic resistivity has to be expected from these qualitative arguments for Co-Pt com-

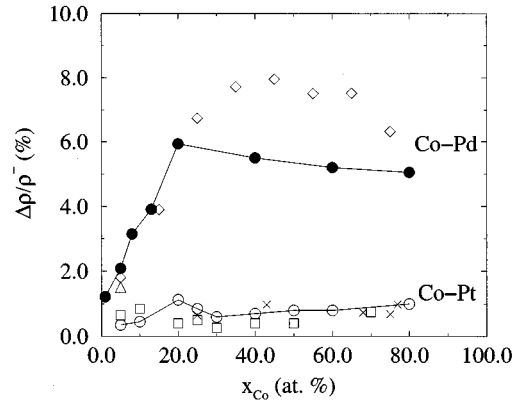


FIG. 5. Calculated spontaneous magnetoresistance anisotropy (SMA) ratio  $\Delta\rho/\bar{\rho}$  of Co-Pd (●) and Co-Pt (○) alloys. Experimental values for Co-Pd were taken from Ref. 12 (△) and Refs. 23 and 24 (◇); for Co-Pt from Refs. 14 (□) and 25 (⊗).

pared to that of Co-Pd (see also the discussion in Sec. III C 1).

## 2. Spontaneous resistance anisotropy

The anisotropy ratios (SMA) calculated from the transverse and longitudinal resistivities are shown in Fig. 5 for the two alloy systems Co-Pd and Co-Pt. Experimental values for both systems are included for comparison.

Co-Pd shows remarkably high SMA values of more than 6% for concentrations higher than 20 at. % Co.<sup>12,23</sup> The calculations reproduce the increase of the experimental data at low Co concentrations very well. For higher Co concentrations the calculated values are slightly too low. Note that the SMA in Co-Pd is still as large as 1.5% even for very low Co contents,<sup>23,24</sup> which was attributed to local orbital moments on the magnetic sites in Ref. 23. It is difficult to investigate the concentration regime below 1% using the KKR-CPA because of the numerical difficulties encountered as one approaches the pure system limit. Nevertheless, the calculated SMA value for 1% Co (1.2%) is in reasonable agreement with experiment.

Co-Pd and Co-Pt show quite a different behavior with respect to the SMA despite their similar electronic structure. In contrast to Co-Pd the SMA for Co-Pt was found to be below 1% throughout the whole concentration range.<sup>14,25</sup> These findings are perfectly reproduced by the relativistic calculation which reflects the slowly varying SMA in Co-Pt. An explanation for this difference shall be given in Sec. III C.

## C. Scalar-relativistic calculations

The fully relativistic calculations presented above include all effects of spin-orbit interaction and spin polarization, and therefore lead to a very reliable description of the anisotropy phenomena in context of transport properties. They are very elegant because no assumptions regarding the nature of scattering, as for example spin conservation, and the relative importance of the various relativistic effects have to be made.

In contrast to this, the discussion of spontaneous resistance anisotropy was mostly based on the two-current model

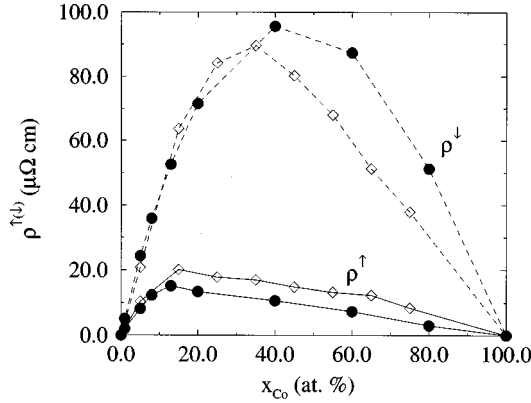


FIG. 6. Subband resistivities  $\rho^\uparrow$  and  $\rho^\downarrow$  for Co-Pd. Solid circles: calculated, open symbols: determined from experimental data by Jen (Ref. 12).

in the past. It leads to the definition of spin-dependent subband resistivities  $\rho^\uparrow$  and  $\rho^\downarrow$ , which do not occur in the rigorous relativistic theory. Such an artificial decomposition of the total resistivity is in general done on the basis of experimentally observed deviations from Matthiessen's rule for nonzero temperatures or of experimental data for ternary alloys.<sup>26</sup> In addition, this model was used as the starting point for resistivity calculations in the framework of transport theories for alloys. Early calculations of this type were, e.g., performed by Brouers, and coworkers<sup>27</sup> and later in a more rigorous way by Akai.<sup>28</sup> Naturally, because of restrictions of the chosen approaches as well as technical ones, the agreement with measured subband resistivities was not that good. With the method presented here, however, much more reliable calculations of the subband resistivities can be carried out. For this purpose, a set of scalar-relativistic calculations was performed based on the same potentials and Fermi energies as used for the relativistic calculations. Adopting the scalar-relativistic approach, the spin-orbit coupling was ignored, while all other relativistic effects have been accounted for. As a consequence, any spin hybridization and any scattering events that lead to a spin flip were omitted, allowing to treat each spin subband system independently. For these reasons, each spin subband appears like a paramagnetic system, and the single subband resistivity tensors do not show the anisotropy expressed by Eq. (1).

### 1. Subband resistivities

The results for the subband resistivities  $\rho^\uparrow$  and  $\rho^\downarrow$  are shown in Fig. 6 for the alloy system Co-Pd, and in Fig. 7 for Co-Pt.

As can be seen for all the alloy compositions of Co-Pd, the condition  $\rho^\downarrow > \rho^\uparrow$  holds with  $\rho^{\uparrow(\downarrow)}$  the partial resistivity for the majority- (minority-) spin system. The majority-spin resistivity takes its maximum value at 13% Co, whereas the minority-spin resistivity has its highest value at 40% Co. The absolute magnitude of resistivity is much higher in the minority spin band, a feature which Co-Pd has in common, e.g., with most nickel alloys.<sup>26</sup> The reason for this can again be traced back to the phase shifts of the *d* electrons (Fig. 4). As a consequence of the very similar behavior of this quantity for the majority-spin system for both components, the scat-

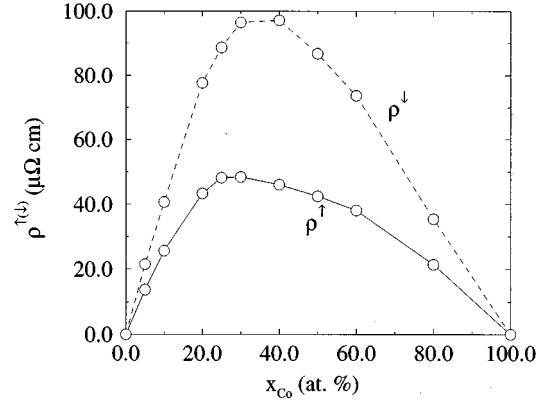


FIG. 7. Calculated subband resistivities  $\rho^\uparrow$  and  $\rho^\downarrow$  for Co-Pt.

tering due to chemical disorder is quite low. This leads to a relative small partial resistivity  $\rho^\uparrow$ . For the minority-spin system, the situation is quite different. Here a strong scattering due to chemical disorder gives rise to a much higher partial resistivity  $\rho^\downarrow$ .

Turning to Co-Pt (Fig. 7), one encounters a similar situation for the minority-spin system. The corresponding partial resistivity is rather high, having its maximum value of almost 100  $\mu\Omega$  cm at about 30–40 % Co. However, although the minority-spin resistivities are quite similar for the two alloy systems Co-Pd and Co-Pt, there is a big difference between the alloys in the majority band, where Co-Pt has a much higher resistivity. The phase shifts shown also for Co-Pt in Fig. 4 immediately provide an explanation for this finding: disorder is much stronger in the spin-up channel of Co-Pt than in Co-Pd due to a much wider separation of the relevant phase-shift resonances. Together with the higher spin-projected DOS  $n^\uparrow(E_F)$  for Co-Pt compared to that of Co-Pd, a higher partial resistivity  $\rho^\uparrow$  results accordingly.

### 2. Discussion in terms of the two-current model

Jen has calculated the subband resistivities of Co-Pd (Ref. 12) from experimental values for the SMA and the residual resistivity by assuming the validity of the two-current model and by using the theory of SMA given by Campbell, Fert, and Jaoul (CFJ).<sup>7</sup> This approach ends with a simple relationship between the isotropic resistivity  $\bar{\rho}$ , SMA ratio  $\Delta\rho/\bar{\rho}$ , and the partial resistivities  $\rho^{\uparrow(\downarrow)}$ :

$$\frac{1}{\bar{\rho}} = \frac{1}{\rho^\uparrow} + \frac{1}{\rho^\downarrow} \quad (6)$$

and

$$\frac{\Delta\rho}{\bar{\rho}} = \gamma \left( \frac{\rho^\downarrow}{\rho^\uparrow} - 1 \right). \quad (7)$$

The phenomenological spin-orbit coupling parameter  $\gamma$  was assumed to be a constant over the entire composition range. Its value was obtained by determining  $\rho^\uparrow$  and  $\rho^\downarrow$  from the measured temperature dependence of the resistivity for the palladium-rich alloy  $\text{Co}_5\text{Pd}_{95}$ , and by investigating the ternary alloy Co-Pd-Ni (see Ref. 11).

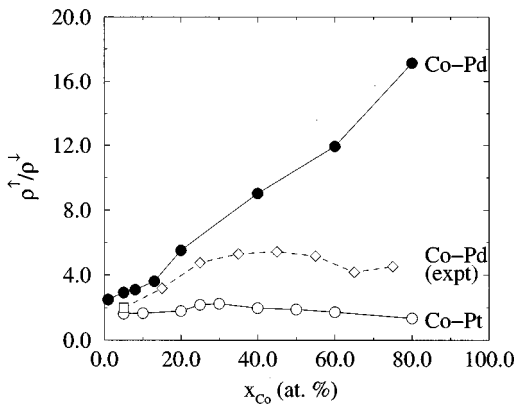


FIG. 8. Ratio of minority and majority resistivity  $\alpha = \rho^\perp / \rho^\parallel$  for Co-Pd (●) and Co-Pt (○) alloys. Measured values for Co-Pd obtained by direct measurement (□) or by extrapolation (◇) (Ref. 11).

Although this procedure seems to be rather crude, the results for the subband resistivities given by Jen (see Fig. 6) agree quite well with the values obtained using the Kubo-Greenwood equation. For high Co contents however, Jen's values for  $\rho^\perp$  are lower, the values for  $\rho^\parallel$  higher than the theoretical resistivities. Therefore, the ratio  $\alpha = \rho^\perp / \rho^\parallel$ , which is apart from  $\gamma$  the central quantity in Eq. (7), is larger for the scalar-relativistic KKR-CPA calculation than deduced by Jen. The theoretical and experimental values for  $\alpha$  values are compared with each other in Fig. 8.

It is important to note that the calculated ratio  $\alpha$  is quite close to the one determined experimentally for  $\text{Co}_5\text{Pd}_{95}$  ( $\alpha \approx 2$ ). For Co-rich Co-Pd, however, the calculated  $\alpha$ 's are much larger than the experimental ones. Because  $\alpha$  was determined directly for  $\text{Co}_5\text{Pd}_{95}$  only, whereas its value for other compositions was determined assuming a constant spin-orbit coupling constant  $\gamma$  derived from this  $\alpha$ , the major reasons for the deviation seem to be the following. First of all one has to keep in mind that Eqs. (6) and (7) were derived for diluted alloys.<sup>7</sup> Their application to concentrated alloys therefore seems to be questionable. Furthermore, there is no justification for taking  $\gamma$  to be concentration independent. Originally, this quantity was meant to represent the spin-orbit coupling strength for the component with the higher concentration.

With the theoretical data for  $\alpha$  (Fig. 8) and the SMA ratio  $\Delta\rho/\bar{\rho}$  (Fig. 5) available, the parameter  $\gamma$  can be obtained using Eq. (7) in a straightforward way. Corresponding results are shown in Fig. 9. In addition, values for  $\gamma$  are given that have been obtained from the theoretical data for  $\alpha$  and the experimental one for the SMA from Fig. 5. As one can see for both data sets, the calculated parameter  $\gamma$  is far from being constant and much smaller than the value used by Jen.<sup>12</sup> As can be seen in Fig. 9, the parameter  $\gamma$  has a maximum at around 13% Co and decreases monotonously with increasing Co content from about 0.015 to 0.04. Although the numerical results differ somewhat, these gross features obviously apply to both data sets.

Turning back to the ratio  $\alpha$  in Fig. 8, one notes that even for 1% Co  $\alpha$  is far away from the value expected for a paramagnetic system ( $\alpha = 1$ ). This shows that even for dilute Co-Pd alloys exchange splitting is strong enough to produce

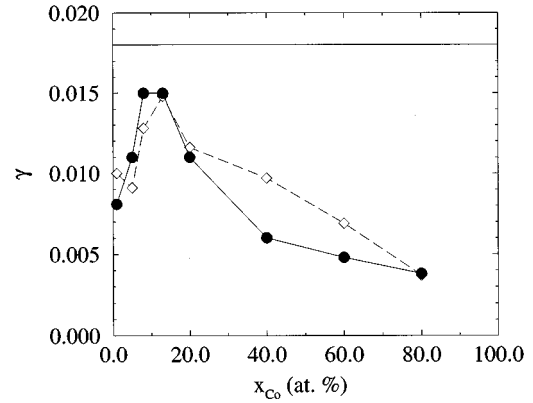


FIG. 9. Spin-orbit coupling parameter  $\gamma$  for Co-Pd calculated according to the CFJ theory [Eqs. (6) and (7)]. Using the theoretical values for  $\rho^\perp / \rho^\parallel$  and for  $\Delta\rho/\bar{\rho}$  the theoretical (●) or the experimental (◇) ones, respectively. In addition, the constant value for  $\gamma$  used by Jen (Ref. 11) is given.

different subband resistivities. In experiments, however, this effect would be masked by contributions to the resistivity which do not depend on the spin direction (such as thermal contributions or nonmagnetic impurities and lattice imperfections) and which become increasingly important as one approaches the pure system Pd.

The ratio  $\alpha$  for Co-Pt is much smaller than that for Co-Pd for all concentrations. This of course reflects the fact that the majority-spin resistivity for Co-Pt is much higher than that of Co-Pd.

One can calculate a spin-orbit coupling parameter  $\gamma$  for Co-Pt in the same way as for Co-Pd using the calculated  $\alpha$ 's and either calculated or measured values for  $\Delta\rho/\bar{\rho}$ . Because the scatter of  $\Delta\rho/\bar{\rho}$  as a function of composition is fairly large for both cases, reflecting the difficulty in accurately determining the small differences between  $\rho^\perp$  and  $\rho^\parallel$  by experiment or calculation, the calculated  $\gamma$  scatters in the same way. The values obtained, however, are in the same range as for Co-Pd, i.e., decreasing from 0.015 on the Pt-rich side to 0.005 on the Co-rich side. This again shows that  $\gamma$  is far from being constant. In addition, the fact that  $\gamma$  is very close to the data for Co-Pd sheds some doubt on the physical meaning of this parameter. If there were a direct connection with the average spin-orbit coupling strength, one would expect  $\gamma$  to be noticeably higher for Co-Pt than for Co-Pd. The only feature that is in line with this expectation is the monotonous decrease of  $\gamma$  for Co concentrations above 13%.

Having determined values for the parameters  $\alpha$  and  $\gamma$  occurring in the CFJ theory [Eqs. (6) and (7)], one can try to interpret the findings for Co-Pd and Co-Pt in terms of this theory. The major consequence of Eqs. (6) and (7) is that there are two conditions which have to be satisfied to obtain a high anisotropy of the electrical resistivity. The first is the presence of strong spin-orbit coupling, which allows electrons to change their spin orientation while they propagate through the crystal or are scattered at lattice sites. The probability of these processes is represented by the parameter  $\gamma$ . These effects are also present in paramagnetic alloys, but do not cause any anisotropy of the transport coefficients because a second condition is required to give rise to the SMA or the anomalous Hall resistivity: if the subband resistivities

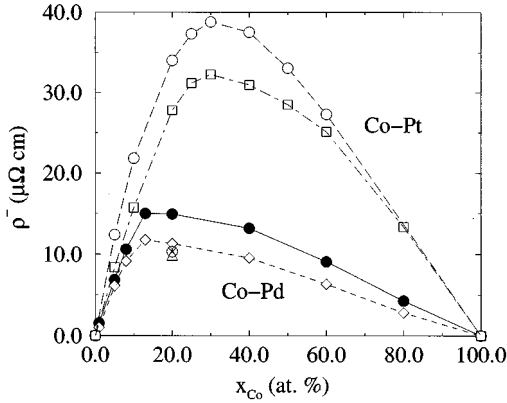


FIG. 10. Residual isotropic resistivity  $\bar{\rho}$  of disordered Co-Pd and Co-Pt alloys. Circles: fully relativistic calculations; squares and diamonds: calculations in the framework of the two-current model ( $\bar{\rho}_{2c}$ ). Relativistic calculations for  $\text{Co}_{20}\text{Pd}_{80}$  with the spin-orbit coupling turned off ( $\Delta$ ) or with a high value for the speed of light ( $\otimes$ ).

$\rho^\perp$  and  $\rho^\uparrow$  are different, as expressed by their ratio  $\alpha$ , the spin transitions and the hybridization of states transfer some of the resistivity from the subband with the higher resistivity to the band with the lower one, and cause a pronounced change of the total isotropic resistivity. Because of the anisotropy of this transfer, the SMA results. In the case of Co-Pd and Co-Pt the parameter  $\gamma$  for the two-alloy system is similar, but the lower degree of disorder in the majority-spin band of Co-Pd makes the spin-orbit scattering more effective in this alloy and causes an SMA, which is for some compositions up to six times larger in Co-Pd than in Co-Pt.

### 3. Isotropic resistivity

In the two-current model without any spin mixing, the subband resistivities can be added up to the total isotropic resistivity according to Eq. (6) (parallel circuits). In the following, the corresponding result will be denoted  $\bar{\rho}_{2c}$ . If the two-current model were valid,  $\bar{\rho}_{2c}$  would be similar to the total resistivity  $\bar{\rho}$ , calculated relativistically, because  $\bar{\rho}_{2c}$  contains all influences present in the relativistic calculation except those due to the spin-orbit interaction. Any difference between  $\bar{\rho}_{2c}$  and  $\bar{\rho}$  can therefore be ascribed to spin-orbit related effects which go beyond the two-current model. Figure 10 shows the two quantities in comparison.

One sees that the relativistic result for  $\bar{\rho}_{2c}$  agrees with  $\bar{\rho}$  quite well. For both alloy systems the two-current calculation yields the asymmetrical resistivity curve also observed for the relativistic calculations and for the experimental resistivities. In both cases, however, the results based on the two-current model are slightly smaller than the resistivities calculated relativistically, indicating that there is some extra resistivity induced by the coupling of the two spin systems via spin-orbit interaction. The relative difference between relativistic and two-current calculations is larger for Co-Pd than for Co-Pt.

Based on the properties of the partial resistivities  $\rho^{\uparrow(\downarrow)}$  for these systems, one concludes that the two-current model works better the smaller the difference between  $\rho^\uparrow$  and  $\rho^\perp$  is. This is completely in line with our previous results for

$\text{Fe}_{20}\text{Ni}_{80}$ .<sup>10</sup> For this alloy an extremely pronounced difference of the partial resistivities occurs. As a consequence inclusion of spin-orbit coupling is essential for this alloy,<sup>10</sup> because omission of the spin-orbit interaction reduces the resistivity to less than one third of its original value.

### D. Relativistic model calculations

In order to show explicitly that relativistic effects are responsible for the observed resistivity differences shown in Fig. 10, we performed relativistic model calculations based on two different manipulations.<sup>10</sup> In a first calculation the speed of light  $c$  was set to a value eight times higher than the correct value  $c_0$  ( $c_0 = 274$  in atomic units) in an arbitrary manner. Because all leading relativistic effects—such as the mass velocity, Darwin, and spin-orbit coupling terms—scale according to  $1/c^2$  with the speed of light, this setting should give rise to results corresponding to the nonrelativistic limit. In a second calculation the spin-orbit interaction was “turned off” by manipulating the Dirac equation following a method described in Ref. 29.

These two types of calculations were applied to the alloy  $\text{Co}_{20}\text{Pd}_{80}$ , with the resulting resistivities shown in Fig. 10. Both values are very close to each other, and similar to the result obtained from the two-current model. Obviously, the suppression of all relativistic influences or spin-orbit effects reduces the resistivity to about 70% of its relativistically correct value. The nearly identical values for the two manipulations show that indeed the spin-orbit interaction is responsible for the resistivity difference, and that other relativistic effects are only of minor importance.

## IV. CONCLUSIONS

In conclusion, the fully relativistic spin-polarized KKR-CPA in conjunction with the Kubo-Greenwood theory for electrical conduction allowed for a rigorous and parameter-free calculation of the anisotropical resistivity in disordered Co-Pd and Co-Pt alloys. The agreement with experiment is very satisfying. Two current calculations allow us to use and test the theory of Campbell, Fert, and Jaoul. It is seen that the basic message of this theory is correct: the resistance anisotropy is promoted by two mechanisms, the spin-orbit interaction and the difference between spin-up and spin-down resistivities. In this picture, the two-alloy systems Co-Pd and Co-Pt have similar levels of spin-orbit-induced scattering, but the higher ratio of  $\rho^\perp/\rho^\uparrow$  for Co-Pd causes the much higher resistance anisotropy for this alloy. However, despite the success of the two-current model it is seen that accurate values for the total resistivity require relativistic calculations.

### ACKNOWLEDGMENT

This work was funded by the Deutsche Forschungsgemeinschaft (DFG) within the programme *Theorie relativistischer Effekte in der Chemie und Physik schwerer Elemente*.

- <sup>1</sup>T.R. McGuire and R.I. Potter, IEEE Trans. Magn. **11**, 1018 (1975).
- <sup>2</sup>J. Banhart and H. Ebert, Europhys. Lett. **32**, 517 (1995).
- <sup>3</sup>O. Jaoul, I.A. Campbell, and A. Fert, J. Magn. Magn. Mater. **5**, 23 (1977).
- <sup>4</sup>F.W. Gorter, J.A.L. Portuigiesser, and D.L.A. Tjaden, IEEE Trans. Magn. **10**, 899 (1974).
- <sup>5</sup>K.J.M. Eijkel and J.H.J. Fluitman, IEEE Trans. Magn. **26**, 311 (1990).
- <sup>6</sup>J. Smit, Physica **16**, 612 (1951).
- <sup>7</sup>I.A. Campbell, A. Fert, and O. Jaoul, J. Phys. C **3**, S95 (1970).
- <sup>8</sup>I.A. Campbell, J. Phys. F **4**, L181 (1974).
- <sup>9</sup>I. Mertig, R. Zeller, and P. Dederichs, Phys. Rev. B **47**, 16 178 (1993).
- <sup>10</sup>J. Banhart, A. Vernes, and H. Ebert, Solid State Commun. **98**, 129 (1996).
- <sup>11</sup>S.U. Jen, T.P. Chen, and S.A. Chang, J. Appl. Phys. **70**, 5831 (1991).
- <sup>12</sup>S.U. Jen, Phys. Rev. **45**, 9819 (1992).
- <sup>13</sup>S.U. Jen, B.L. Chao, and C.C. Liu, J. Appl. Phys. **76**, 5782 (1994).
- <sup>14</sup>S.U. Jen, T.P. Chen, and B.L. Chao, Phys. Rev. **48**, 12 789 (1993).
- <sup>15</sup>D.A. Greenwood, Proc. Phys. Soc. London **71**, 585 (1958).
- <sup>16</sup>W.H. Butler, Phys. Rev. B **31**, 3260 (1985).
- <sup>17</sup>J.C. Swihart, W.H. Butler, G.M. Stocks, D.M. Nicholson, and R.C. Ward, Phys. Rev. Lett. **57**, 1181 (1986).
- <sup>18</sup>J. Banhart, H. Ebert, J. Voitländer, and P. Weinberger, Phys. Rev. B **50**, 2104 (1994).
- <sup>19</sup>H. Ebert, B. Drittler, and H. Akai, J. Magn. Magn. Mater. **104-107**, 733 (1992).
- <sup>20</sup>V.L. Moruzzi, J.F. Janak, and A.R. Williams, *Calculated Electronic Properties of Metals* (Pergamon, New York, 1978).
- <sup>21</sup>G.M. Stocks, W.M. Temmerman, and B.L. Gyorffy, in *Electrons in Disordered Metals and at Metallic Surface*, edited by P. Phariseau, B. L. Gyorffy, and L. Scheire (Plenum, New York, 1979), p.193.
- <sup>22</sup>C.M. Hurd, S.P. McAllister, and C. Couture, J. Appl. Phys. **50**, 7531 (1979).
- <sup>23</sup>S. Senoussi, I.A. Campbell, and A. Fert, Solid State Commun. **21**, 269 (1977).
- <sup>24</sup>A. Hamzić, S. Senoussi, I.A. Campbell, and A. Fert, J. Phys. F **8**, 1947 (1978).
- <sup>25</sup>T.R. McGuire, J.A. Aboaf, and E. Klokholm, J. Appl. Phys. **55**, 1951 (1984).
- <sup>26</sup>J.W.F. Dorleijn, Philips Res. Rep. **31**, 287 (1976).
- <sup>27</sup>F. Brouers, A.V. Vedyayev, and M. Giorgino, Phys. Rev. B **7**, 380 (1973).
- <sup>28</sup>H. Akai, Physica B & C **86-88B**, 539 (1977).
- <sup>29</sup>H. Ebert, H. Freyer, A. Vernes, and G.-Y. Guo, Phys. Rev. B **53**, 7721 (1996).